Article

Deciphering the depositional environment of the laminated Crato fossil beds (Early Cretaceous, Araripe Basin, North-eastern Brazil)

HEIMHOFER, Ulrich, *et al*.

HEIMHOFER, Ulrich, *et al*. Deciphering the depositional environment of the laminated Crato fossil beds (Early Cretaceous, Araripe Basin, North-eastern Brazil). *Sedimentology*, 2010, vol. 57, no. 2, p. 677-694

DOI : 10.1111/j.1365-3091.2009.01114.x

SEDIMENTOLOGY the journal of the International Association of Sedimentologists

Sedimentology (2010) **57,** 677–694 doi: 10.1111/j.1365-3091.2009.01114.x

Deciphering the depositional environment of the laminated Crato fossil beds (Early Cretaceous, Araripe Basin, North-eastern Brazil)

ULRICH HEIMHOFER*, DANIEL ARIZTEGUI†, MARC LENNIGER*, STEPHEN P. HESSELBO‡, DAVID M. MARTILL§ and ARISTOTELES M. RIOS-NETTO¶

**Institute for Geology, Mineralogy and Geophysics, Ruhr-University Bochum, 44801 Bochum, Germany (E-mail: ulrich.heimhofer@rub.de)*

†*Section of Earth Sciences, University of Geneva, 1205 Geneva, Switzerland*

‡*Department of Earth Sciences, University of Oxford, Oxford OX1 3PR, UK*

§*School of Earth and Environmental Sciences, University of Portsmouth, Portsmouth PO1 3QL, UK*

¶*Department of Geology, IGEO, UFRJ, Ilha do Fundão, 21.949-900, Rio de Janeiro, Brazil*

Associate Editor – Tracy Frank

ABSTRACT

The laminated limestones of the Early Cretaceous Crato Formation of the Araripe Basin (North-eastern Brazil) are world-famous for their exceptionally well-preserved and taxonomically diverse fossil fauna and flora. Whereas the fossil biota has received considerable attention, only a few studies have focused on the sedimentary characteristics and palaeoenvironmental conditions which prevailed during formation of the Crato *Fossil Lagerstätte*. The Nova Olinda Member represents the lowermost and thickest unit (up to 10 m) of the Crato Formation and is characterized by a pronounced rhythmically bedded, pale to dark lamination. To obtain information on palaeoenvironmental conditions, sample slabs derived from three local stratigraphic sections within the Araripe Basin were studied using high-resolution multiproxy techniques including detailed logging, petrography, μ-XRF scanning and stable isotope geochemistry. Integration of lithological and petrographic evidence indicates that the bulk of the Nova Olinda limestone formed via authigenic precipitation of calcite from within the upper water column, most probably induced and/or mediated by phytoplankton and picoplankton activity. A significant contribution from a benthonic, carbonate-secreting microbial mat community is not supported by these results. Deposition took place under anoxic and, at least during certain episodes, hypersaline bottom water conditions, as evidenced by the virtually undisturbed lamination pattern, the absence of a benthonic fauna and by the occurrence of halite pseudomorphs. Input of allochthonous, catchment-derived siliciclastics to the basin during times of laminite formation was strongly reduced. The $\delta^{18}O$ values of authigenic carbonate precipitates (between −7·1 and −5·1‰) point to a ^{18}O-poor meteoric water source and support a continental freshwater setting for the Nova Olinda Member. The $\delta^{13}C$ values, which are comparatively rich in ^{13}C (between −0·1 and +1·9‰), are interpreted to reflect reduced throughflow of water in a restricted basin, promoting equilibration with atmospheric CO_2, probably in concert with stagnant conditions and low input of soil-derived carbon. Integration of lithological and isotopic evidence indicates a shift from closed to semi-closed conditions towards a more open lake system during the onset of laminite deposition in the Crato Formation.

Keywords Authigenic calcite, Crato Formation, fossil lagerstätte, lacustrine, stable isotopes, μ-XRF scanning.

INTRODUCTION

Lake deposits are often associated with an extraordinary wealth of well-preserved fossil biota and offer important insights into past fauna and flora. Famous examples of *Fossil Lagerstätten* formed under lacustrine conditions include the Messel oil shale in Germany, the Florissant Formation in Colorado, USA, the Jehol Biota in North-eastern China and the Las Hoyas Basin in East-central Spain (Franzen & Michaelis, 1988; Fregenal-Martínez & Meléndez, 1994; Zhou *et al.*, 2003; Meyer & Smith, 2008). For the Mesozoic of Gondwana, the Crato fossil beds of the Araripe Basin, located in North-eastern Brazil, represent one of the most productive non-marine fossil sites. Here, a diverse insect and vertebrate fauna of Early Cretaceous age is preserved within rhythmically laminated limestones (LL) of probable lacustrine origin. To date, more than 100 insect species, nine species of fish and nearly a dozen pterosaurs, turtles and lizards have been reported from the Crato Formation (for a comprehensive overview see Martill *et al.*, 2007a). The fossils are remarkable for their concentrated abundance, as well as for their exceptional preservation, which occurs in the form of mineralized replications. Preservation of delicate structures like antennae, compound eyes and colour patterns of insect wings, as well as soft tissue associated with vertebrate remains, has been reported (Martill & Frey, 1995; Martill & Davis, 2001; Menon & Martill, 2007). The fossil fauna and flora of the Nova Olinda limestone (the basal member of the Crato Formation) is considered to be predominantly allochthonous with most of the fossils being blown-in by the wind or washed-in by one of the rivers draining the hinterland (Menon & Martill, 2007).

The high-fidelity preservation of the Crato fossils suggests that deposition and fossilization of the various organisms occurred under extraordinary depositional conditions. Since their first mention by Gardner (1846), the Crato laminites have attracted a multitude of palaeontological studies dealing predominantly with the systematics and taxonomy of the diverse biota. However, despite the importance of this famous fossil site for the understanding of Early Cretaceous low-latitude ecosystems, detailed information on the depositional environment is relatively scarce. Exceptions include studies of the organic matter composition (Baudin & Berthou, 1996; Neumann *et al.*, 2003) and of particular sedimentary features (Martill *et al.*, 2007b, 2008). Some workers have examined spot samples from the Crato Formation in studies on the Araripe Group as a whole (Berthou *et al.*, 1990) and limited assessments of the palaeoenvironment have been undertaken (Cavalcanti & Vianna, 1990; Martill & Wilby, 1993). However, many fundamental issues with regard to the depositional history of these famous fossil-hosting limestones still remain unsolved.

In this study, the laminites of the Nova Olinda Member are investigated with an integrated approach combining detailed petrographic analysis with high-resolution μ-XRF scanning and stable isotope geochemistry. The main objectives are: (i) deciphering the source of the fine-grained carbonate, which acts as an embedding agent for the fossil biota; (ii) investigating the nature of the lamination pattern; and (iii) providing a better understanding of the palaeoenvironmental conditions prevailing during the formation of the Crato fossil beds.

GEOLOGICAL SETTING

The Araripe Basin represents a fault-bound interior sedimentary basin, located in the border area of the States of Piauí, Ceará and Pernambuco in North-eastern Brazil (Fig. 1A and B). The sedimentary evolution of this intracratonic rift basin was strongly controlled by extensional tectonics accompanying the opening of the southern and equatorial branches of the South Atlantic rift system during the Early Cretaceous (Chang *et al.*, 1988; de Matos, 1999) (Fig. 1C). In the Cariri valley, NW-SE directed extension resulted in the reactivation of pre-existing sigmoidal shear zones and generated a suite of NE-SW trending half-grabens including the Araripe, Rio do Peixe and Iguatu Basins (de Matos, 1999). In the Araripe Basin, gravity, magnetic and seismic data indicate the occurrence of two sub-basins, the Feira Nova in the east and the Crato sub-basin in the west which are both bound by NE-trending normal faults (Ponte & Ponte Filho, 1996). With the cessation of extension during the Aptian, the North-eastern Brazilian rift

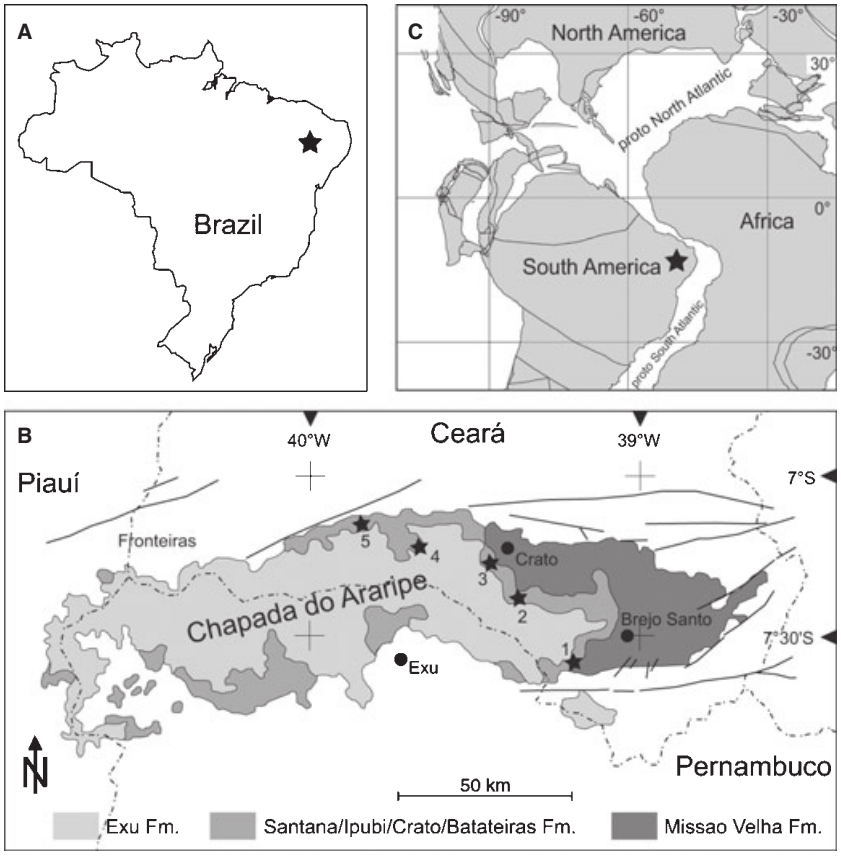

Fig. 1. (A) Map of Brazil showing the location of the Araripe Basin in the north-east. (B) Simplified geological map of the Araripe Basin. Asterisks mark the location of sections with: '1' Sobradinho; '2' Caldas; '3' Crato Cascata; '4' Nova Olinda and; '5' Tatajuba. (C) Plate tectonic reconstruction showing the position of the Araripe Basin during the late Early Cretaceous (*ca* 120 Ma). Map modified after Geomar map generator (http://www.odsn.de).

basins entered the transitional post-rift phase. Above a major unconformity representing a significant hiatus (Coimbra *et al.*, 2002), the post-rift stage of the Araripe Basin is represented by the deposits of the Araripe Group covering Late Aptian to Early Albian. During this stage, low subsidence resulted in the deposition of deltaic to lacustrine sediments (Rio da Batateiras and Crato Formations) followed by evaporites (Ipubi Formation) and marginal marine shales (Romualdo and Arajara Formations). Above a major unconformity, the Araripe Group is overlain by a massive succession of fluvial siliciclastics of most probably post-Albian age (Exu Formation) (Ponte & Appi, 1990).

The Crato Formation itself consists of several units of LL interbedded with a series of claystones, siltstones and sandstones (Fig. 2). According to Martill & Heimhofer (2007), the Crato Formation can be divided into four different members including from bottom to top: the Nova Olinda, Caldas, Jamacaru and Casa de Pedra Members (Fig. 3). The focus of the present study is the laminated carbonates of the Nova Olinda Member which represent the lowermost and thickest limestone horizon and host the famous Crato *Fossil Lagerstätte*. These limestones are characterized by a conspicuous lamination, which is laterally very consistent and can be traced along several tens of metres in outcrop (Fig. 2A). Similarly, the vertical stacking pattern shows very regular rhythmical bedding. Based on differences in lithological composition and style of lamination, Neumann *et al.* (2003) distinguish between two types of laminated carbonate facies: (i) clay–carbonate rhythmites (CCR) facies are represented by very fine laminated, ochre-brown marly limestones with a variable detrital component (Fig. 2B); and (ii) LL facies represents the typical, fossil-rich 'plattenkalk' of the Nova Olinda Member with its distinct and very regular dark-grey to brown to white banding. Macroscopically well-preserved 'blue' LL facies accounts for the bulk of the Nova Olinda limestone and is the main target for quarrying (Fig. 2C).

The Nova Olinda Member crops out between Tatajuba in the north-west of the Chapada do

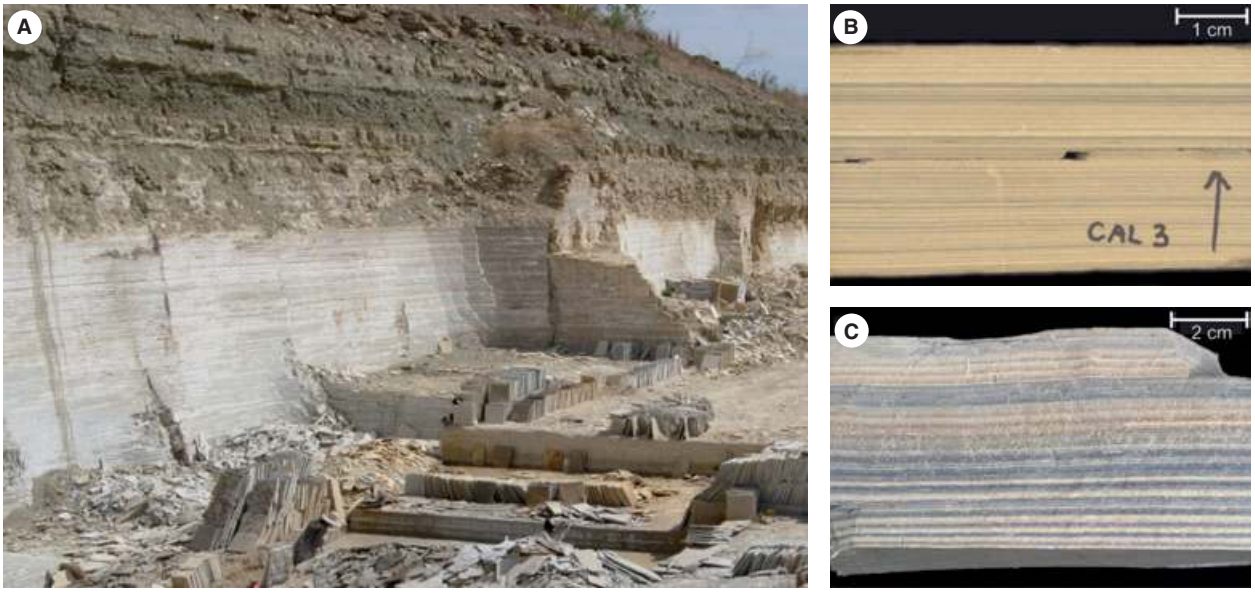

Fig. 2. (A) View of the Nova Olinda Member exposure in one of numerous quarries located between Nova Olinda and Santana do Cariri, Ceará, NE Brazil. Here, the sharp contact between the Crato plattenkalk and the claystones, siltstones and sandstones of the overlying Caldas Member is well-exposed. The approximate height of the pale plattenkalk unit is *ca* 6 m. (B) Clay–carbonate rhythmite from the uppermost part of the Nova Olinda Member (sample CAL-3, Caldas section). Note the well-developed fine-scale lamination pattern. (C) Typical 'blue' laminated limestone facies with the distinct planar dark-pale banding from the middle part of the Nova Olinda Member (sample NO-1, Nova Olinda quarry).

Araripe and extends south-eastward to Sobradinho (Fig. 1B), indicating a minimum NW-SE extent to the depositional setting of *ca* 70 km. In the south and south-western part of the Araripe Basin, the relationship with similar facies is not well-established (Martill & Heimhofer, 2007). The LL of the Nova Olinda Member is well-exposed and accessible in numerous quarries along the north-western flank of the Chapada where the Crato 'plattenkalk' is mined as an ornamental paving stone and for cement manufacture between Santana do Cariri and Crato. Good exposures, including the overlying strata, can be found in the quarries of Tatajuba, Nova Olinda and Caldas, and in the river sections near Crato (Crato Cascata) and close to Sobradinho (Fig. 1B). The thickness of the LL unit shows considerable variation and ranges from 6 to 8 m in the Nova Olinda area to up to 10 m at Tatajuba.

Because the absence of age-diagnostic marine macrofossils and microfossils or volcanic ash-beds, the stratigraphic age of the Crato Formation is still a matter of debate. Based on ostracod assemblages and terrestrial palynomorphs and, in consideration of existing studies, Coimbra *et al.* (2002) propose a revised stratigraphic framework for the Early Cretaceous succession of the Araripe Basin. According to this work, the entire Crato Formation is part of the *Sergipea variverrucata* palynozone which implies an Aptian age for the Nova Olinda Member. This stratigraphic assignment is in accordance with a recent study by Batten (2007) which suggests a Late Aptian age for the Crato laminites based on palynological constraints.

During late Early Cretaceous times, the Araripe Basin was located at a palaeolatitude of 10° to 15° south of the equator (Fig. 1C), situated well within the tropical-equatorial hot arid belt of Chumakov *et al.* (1995). The widespread occurrence of evaporites along the evolving South Atlantic rift system, the absence of coal deposits and the dominance of drought-resistant, xerophytic vegetation indicate the predominance of semi-arid to arid climatic conditions in this area (Doyle *et al.*, 1982; Ziegler *et al.*, 2003). According to Arai (2000), global eustatic sea-level rise in the course of the late Early Cretaceous resulted in the episodic establishment of a highly restricted, NE-SW trending epeiric seaway linking the intracratonic Araripe Basin either with the opening northern part of the South Atlantic Ocean (via the Recôncavo, Tucano and Jatoba Basin complex) or the Central Atlantic Ocean (via the Parnaíba or Potiguar Basins). Whereas the influence of marine waters (with strongly fluctuating salinities) has been demonstrated clearly for the Ipubi and Santana Formations, estimates for palaeosalinities during deposition of the Crato Formation are

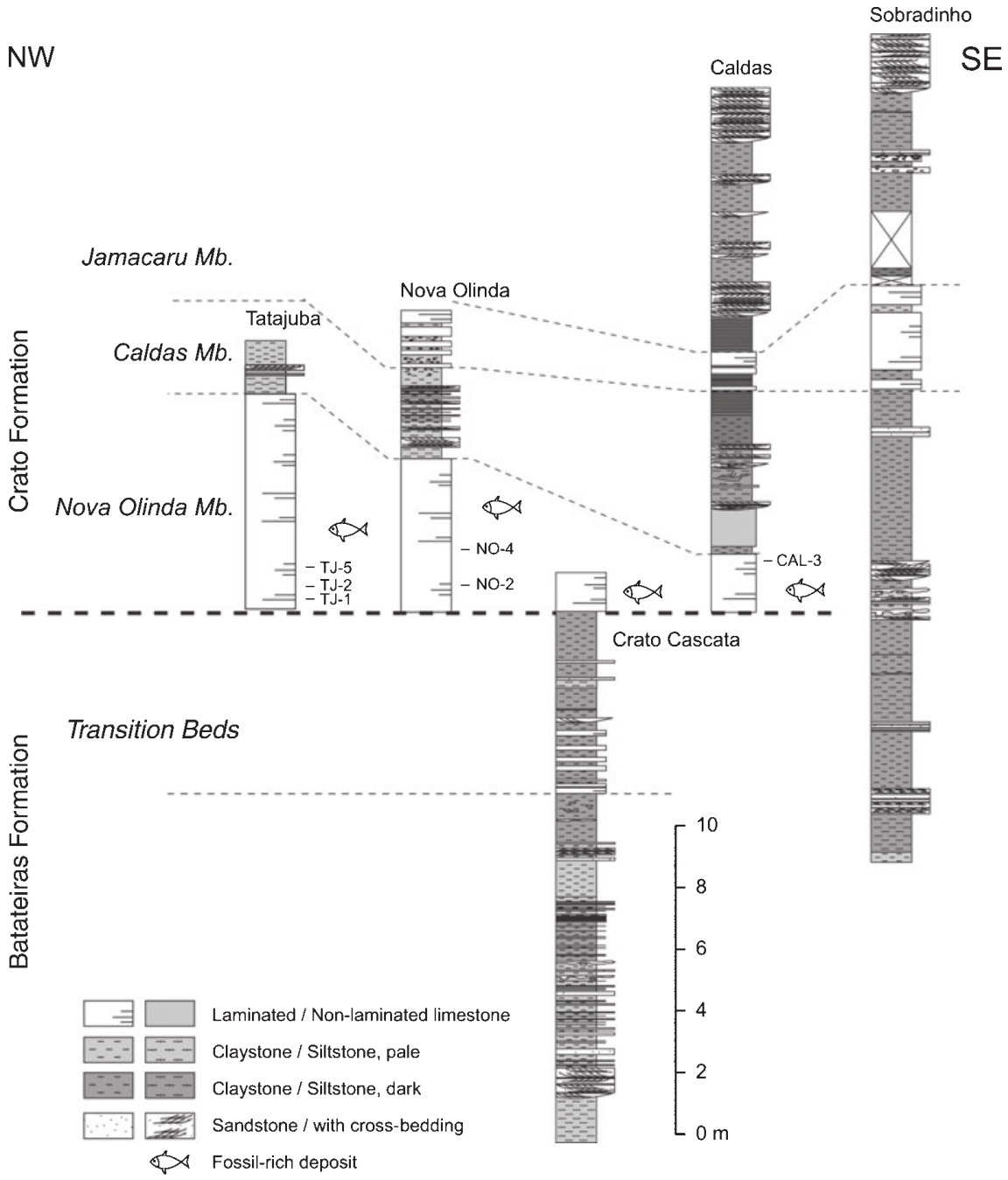

Fig. 3. Lithostratigraphic correlation of sections along a SE to NW trending transect across the Chapada do Araripe. Stratigraphic nomenclature follows Martill & Heimhofer (2007). The base of the Nova Olinda Member serves as a lithostratigraphic datum. The fish symbol marks the fossil-bearing laminite interval of the Nova Olinda Member. Note the position of the individual samples used in this study.

not well-established and still a matter of debate (Neumann *et al.*, 2003; Martill *et al.*, 2007a).

MATERIAL AND METHODS

Material from three different quarries spread along the north-eastern flank of the Chapada do Araripe has been investigated to constrain the spatial and temporal variability of the laminated carbonate facies. Samples from the Tatajuba, Nova Olinda and Caldas quarries were studied and sampling was restricted to the Nova Olinda Member (Fig. 3). Only material from macroscopically well-preserved laminite facies has been used for the different types of analyses. The selected batch of

samples is considered to be representative for the entire Nova Olinda Member.

The CCR facies is well-developed in the uppermost and lowermost part of the Nova Olinda Member in the Caldas and Tatajuba quarries (samples CAL-3 and TJ-1). Well-preserved, non-weathered LL facies is represented by material collected from Nova Olinda quarry (NO-4) and Tatajuba quarry (TJ-2 and TJ-5). For high-resolution $\delta^{13}C$ and $\delta^{18}O$ analyses, three successive laminite slabs (TJ-1, TJ-2 and TJ-5) from Tatajuba have been studied which cover the well-preserved lower part of the section. In addition, a single slab located in the lower part of the Nova Olinda section (sample NO-2) has been investigated for stable isotope analysis (see Fig. 3 for the exact stratigraphic position of these samples).

The morphological features of the laminites were studied using a LEO/Zeiss 1530 Gemini field emission scanning electron microscope (SEM; Carl Zeiss NTS GmbH, Oberkochen, Germany). Freshly broken pieces of sample were mounted on aluminium stubs vertical to bedding for these SEM investigations. The acceleration voltage was 10 and 20 keV at a working distance of *ca* 10 mm. Samples were carbon coated to avoid charging.

Qualitative elementary composition was obtained on selected samples at a micrometre resolution (4 data points/mm) using an EAGLE III X-ray fluorescence (μ-XRF; EDAX Inc., Mahwah, NJ, USA) device under vacuum conditions with a 50 μm diameter beam at the University of Geneva, Switzerland. Three selected limestone slabs were measured for light (Mg, Al, Si, S, Ca, Ti, Mn and Fe) and heavy (Cu, Zn and Sr) elements. The data are expressed as elemental intensities in counts per second (cps). Only Ca, S and Fe are presented here among the total elements determined. Other elements either provide the same information (e.g. Mn) or exhibit counting values that were too low for a reliable interpretation.

Sample material of laminites was collected from polished slabs (*ca* 2·0 mm in thickness) for stable-isotope analyses. Individual laminae were sampled using a Merchantek MicroMill (New Wave Research, Bozeman, MT, USA) equipped with tungsten drill bits (0·4 mm in diameter). Individual laminae were drilled parallel to bedding to obtain sufficient material for stable isotope analyses. Sample powders have been measured using a Finnigan MAT Delta S stable isotope ratio mass spectrometer (Thermo Finnigan MAT GmbH, Bremen, Germany) coupled to a Gasbench II (Thermo Finnigan). External precision was better than ±0·07‰ for $\delta^{13}C$ and ±0·1‰ for $\delta^{18}O$.

RESULTS

Transmitted light and scanning electron microscopy

Clay–carbonate rhythmite facies

Thin-section microscopy allows a clear differentiation between dark and pale laminae with the dark laminae enriched in clay minerals and organic matter. Pale and dark layers form rhythmically developed laminae-couplets between 0·5 and 0·8 mm thick. The sedimentary organic material occurs in bundles of thin, partly anastomosing layers, which show a thickness of *ca* 0·1 mm. These organic-rich layers are associated with finely dispersed pyrite grains. In contrast, the alternating pale laminae are characterized by a dense and homogenous fine-grained texture composed of microcrystalline calcite grains (5 to 10 μm). Bioclastic material is restricted to the scarce occurrence of black, coalified plant debris and rare ostracod carapaces. Angular to subangular quartz grains (up to 0·1 mm) occur regularly and are not confined to certain layers.

Analysis of the ultrastructure under the SEM reveals that the calcite laminae of the CCR facies are composed almost exclusively of idiomorphic calcite rhombohedra and polyhedra with well-developed crystal faces (Fig. 4A and B). Individual crystals show no preferred orientation and only minor interlocking is observed between them. Calcite rhombohedra are generally well-preserved with only a few grains showing irregularly distributed microvugs and microchannels, probably reflecting early dissolution features (Fig. 4B). Besides calcite rhombohedra, small (<5 μm) and friable carbonate aggregates can be observed which lack identifiable crystal shapes. Other components include framboidal pyrite as well as phyllosilicates exhibiting the typical stacking pattern. The absence of typical biogenic fabrics, for example, in form of shell debris, microspheres, tubules or coccoid chains, is noteworthy. The individual crystals are loosely packed, resulting in a relatively high interparticle porosity with pores of irregular morphology (Fig. 4B and C). The absence of a pore-space filling cement phase in the CCR facies is remarkable and results in a microporous crystal framework. Incipient growth of calcite spar is restricted to grain-to-grain contacts (Fig. 4D).

Laminated limestone facies

In thin-section, the LL facies is very fine-grained and shows a homogenous grain-size distribution.

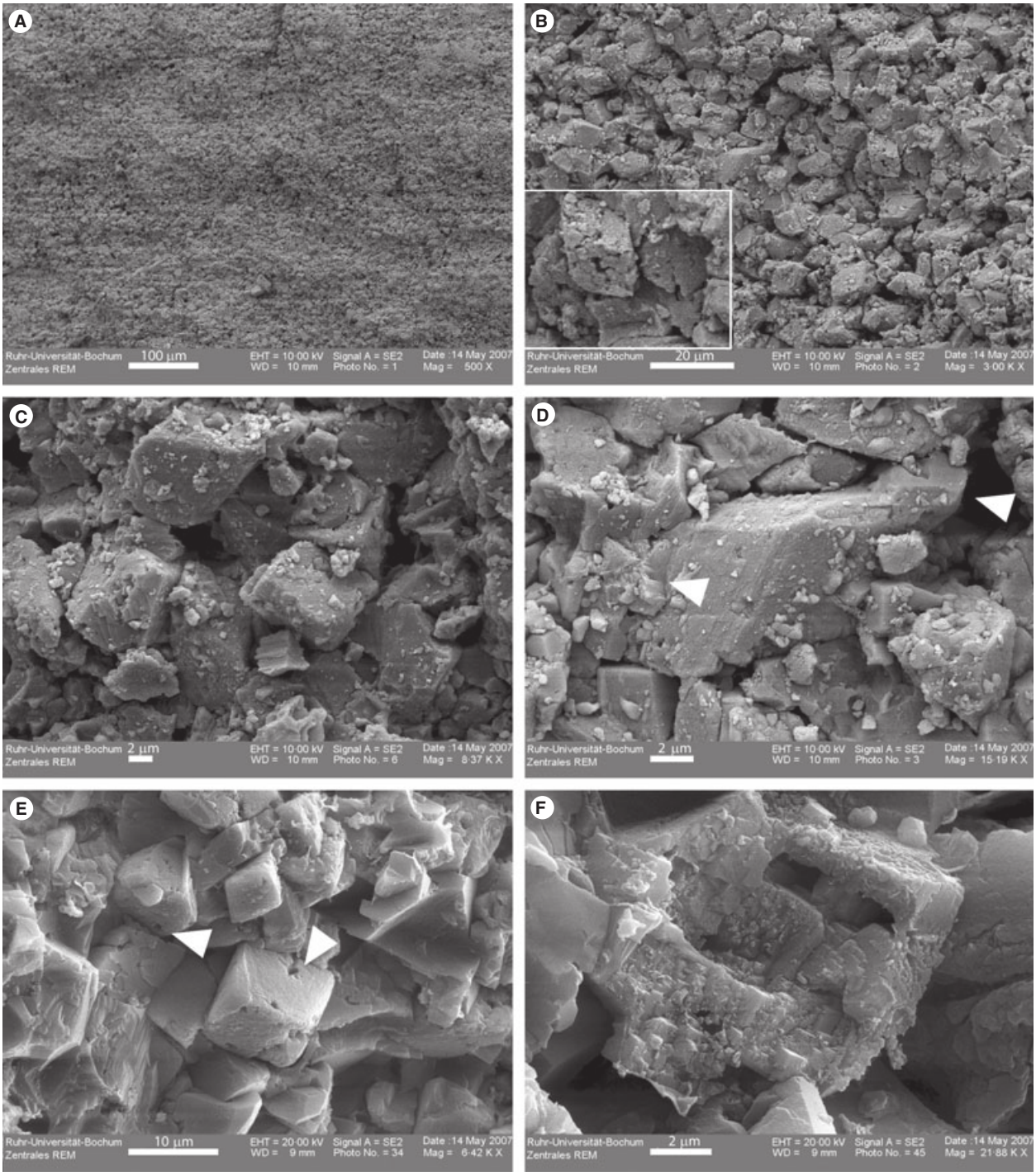

Fig. 4. Comparison of ultrastructure of laminated facies from Tatajuba quarry. (A) View of a freshly broken surface vertical to bedding, showing the homogenous grain-size distribution within the micrite (sample TJ-1, CCR facies). (B) Close-up of clay–carbonate rhythmite exhibiting high interparticle porosity between individual calcite crystals. Note the absence of significant cement infilling between the grains. Inset shows a close-up of calcite rhombohedra with irregular vugs (sample TJ-1, CCR facies). (C) Details of individual crystals. Note the well-developed rhombohedral shape and faces of the crystals. Pore space between individual grains is open (sample TJ-1, CCR facies). (D) Densely packed calcite rhombohedra with incipient cement growth in interparticle cavities (arrows) (sample TJ-1, CCR facies). (E) Laminated limestone facies with parts of the pore space being filled with blocky calcite cement. Arrows indicate dissolution features on calcite crystal faces (samples TJ-2, LL facies). (F) Close-up of a calcite rhombohedra exhibiting skeletal growth resulting in the development of intracrystal porosity (sample TJ-2, LL facies).

Grain size ranges from 5 to 15 μm which places the Nova Olinda plattenkalk in the microspar range *sensu* Folk (1959). Under transmitted light, the lamination pattern is faintly visible and boundaries between dark and pale layers are rather diffuse. Different hierarchies of lamination can be observed with the dominant hierarchy represented by the distinct dark-grey/white couplets. Individual laminae are 2 to 3 mm in thickness, thus resulting in couplets of up to 6 mm. Within dark-grey laminae an irregular sub-lamination can be observed with single layers *ca* 0·2 mm thick. Furthermore, the dark-grey layers are enriched with finely disseminated pyrite. Bioclastic particles represent a minor component and are restricted to the rare occurrence of phosphatic fish remains, ostracod carapaces and isolated terrestrial plant fragments. Detrital material is minor with silt-sized, subangular quartz and K-feldspar grains occurring in accessory amounts. Because of the fine-grained and dense nature of the sedimentary rock, identification of cement phases between the individual grains is limited in thin-section.

Scanning electron microscopic analysis reveals a microtexture similar to the CCR facies and idiomorphic rhombohedra compose the bulk of the carbonate. However, compared with typical CCR facies, LL facies exhibits a higher content of spar and, hence, reduced interparticle porosity. Growth of calcite spar did not occur in optical continuity with the rhombohedra as indicated by abundant casts resulting from the breaking out of calcite crystals and by the fibrous nature of the cement phase (Fig. 4E). In addition, skeletal growth of calcite rhombohedra is a commonly observed feature resulting in the development of intracrystalline pores (Fig. 4F).

Ultra high-resolution μ-XRF-scanning

High-resolution μ-XRF analysis provides a record of geochemical variations on the sub-millimetre scale for the Crato laminites. Three samples representing LL facies (NO-4 and NO-2) and CCR facies (CAL-3), respectively, have been measured with an XRF scanner, which allows for non-destructive analysis of major and minor elements at the surface of cut slabs.

All measured slabs show the strongest intensities, in the order of *ca* 10 000 cps, for Ca; this clearly reflects the high abundance of authigenic calcite which forms the bulk of the Crato limestone. This finding is in accordance with $CaCO_3$ contents in excess of 92 wt% for both limestone facies. In all studied slabs, Ca intensities display a clear correlation with observed colour changes and show a decreasing trend associated with bundles of dark laminae and vice versa. This trend is even more pronounced when looking at the Ca/Fe ratio (Figs 5 and 6). All other elements show intensities in the range of at least one (Fe), or several (Mg, Al, Si, Ti and Sr), orders of magnitude less than Ca. Intensity curves of Fe (*ca* 110 to 3100 cps) and S (*ca* 20 to 220 cps) of the CCR sample show distinct fluctuations in the high frequency pattern (Fig. 5). The two elements display a very similar behaviour (R^2 = 0·61) that generally speaking is opposite to variations in total Ca counts. A clear correlation between colour changes and variations in both Fe and S is evident. Bundles of dark laminae are associated with increasing intensities and vice versa. Indeed, even subtle changes in colour intensity correlate well with comparatively smaller variations in the ratio between the more conservative against most non-conservative elements within this sample (i.e. Ca/Fe ratio). A correlation between Mn and Fe intensities (R^2 = 0·03) is absent in the measured CCR sample.

In the LL facies (sample NO-4), S intensities show a similar range compared with CCR facies and fluctuate between 10 and 250 cps. Variations in the intensity curve of S show a clear correspondence with sediment colour, which is well-expressed in the upper part of slab NO-4, where several dark laminae are reflected in distinct peaks of the S record (Fig. 6). Fluctuations in Fe intensities (200 to 4000 cps) are most pronounced in the rather pale segments in the middle part of the slab and paralleled by prominent peaks in the Ca/Fe ratio. Whereas Fe and Mn show a clear correlation (R^2 = 0·77), no correlation can be observed between Fe and S (R^2 = 0·01).

Stable isotopes

Stable isotope values vary between 1·93 and −0·14‰ for $\delta^{13}C$ and between −5·10 and −7·06‰ for $\delta^{18}O$ within all analysed carbonates. Individual laminite slabs, which have been sampled 'layer by layer' at a high resolution, show a strong clustering of values with only minor internal variability, e.g. slab TJ-1 (n = 19) shows a range of values of 0·28 ± 0·07‰ for $\delta^{13}C$ and 0·47 ± 0·1‰ for $\delta^{18}O$ (Fig. 7). These clustered values derived from the individual slabs do not overlap. None of the measured slabs shows a significant covariance of carbon and oxygen values; correlation

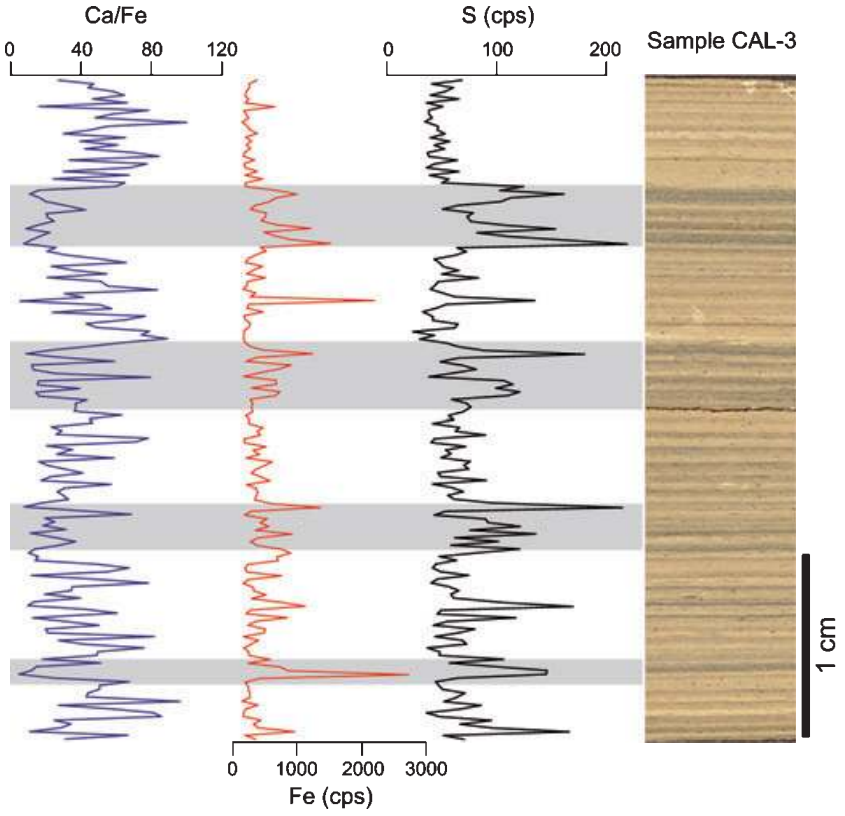

Fig. 5. Ultra high-resolution μ-XRF scanning of a 4 cm slab of CCR facies of the Nova Olinda Member (Mina Caldas quarry). The Ca/Fe ratio and Fe and S intensities (in counts per second, cps) are shown. μ-XRF results are plotted versus slab height; grey bands correspond to visually darker horizons.

coefficients are weak, ranging from +0·29 (NO-4) to +0·10 (TJ-2). Stratigraphic trends in stable-isotope profiles across individual slabs do not show major fluctuations. Variations are restricted to small-scale shifts which are most pronounced in slab TJ-2 (with shifts of up to 0·7‰ in $\delta^{18}O$ between single laminae). No apparent relationship is observed between the colouring of individual layers and their corresponding stable isotope signatures (Fig. 8).

INTERPRETATION AND DISCUSSION

Evaluation of the diagenetic overprint

Lacustrine carbonates are prone to early diagenetic alteration. Early cementation and hardground formation can occur on relatively short time scales as indicated by, for example, the indurated carbonate crusts observed in Holocene shoreline and nearshore deposits of saline maar lakes (Last, 1992). On the other hand, under specific depositional and burial conditions, lacustrine chalks may preserve their primary texture and mineralogy for millions of years (Arribas *et al.*, 2004). To extract a palaeoenvironmental signal from the laminites of the Nova Olinda Member, possible effects due to early or late diagenetic overprint must be identified and differentiated from an original signature.

Thermally immature conditions of sedimentary organic matter derived from the Crato Formation have been reported by Baudin & Berthou (1996) based on pyrolysis data. The colour of palynomorphs (thermal alteration index <2 after Staplin, 1982) and the occurrence of intact, thin-walled angiosperm pollen provide further evidence for the generally low degree of thermal alteration and exclude deep burial of these deposits. These observations are in line with the results from petrographic inspection of the Nova Olinda laminites. Typical burial diagenetic features such as recrystallization of calcite, cementation of fractures or formation of stylolites are virtually absent in both types of laminite facies. Inspection of the ultrastructure of the clay-rich CCR facies shows that pore-filling cement phases are rare and restricted to incipient growth between individual crystals. High interparticle porosity, which is considered to represent the original depositional

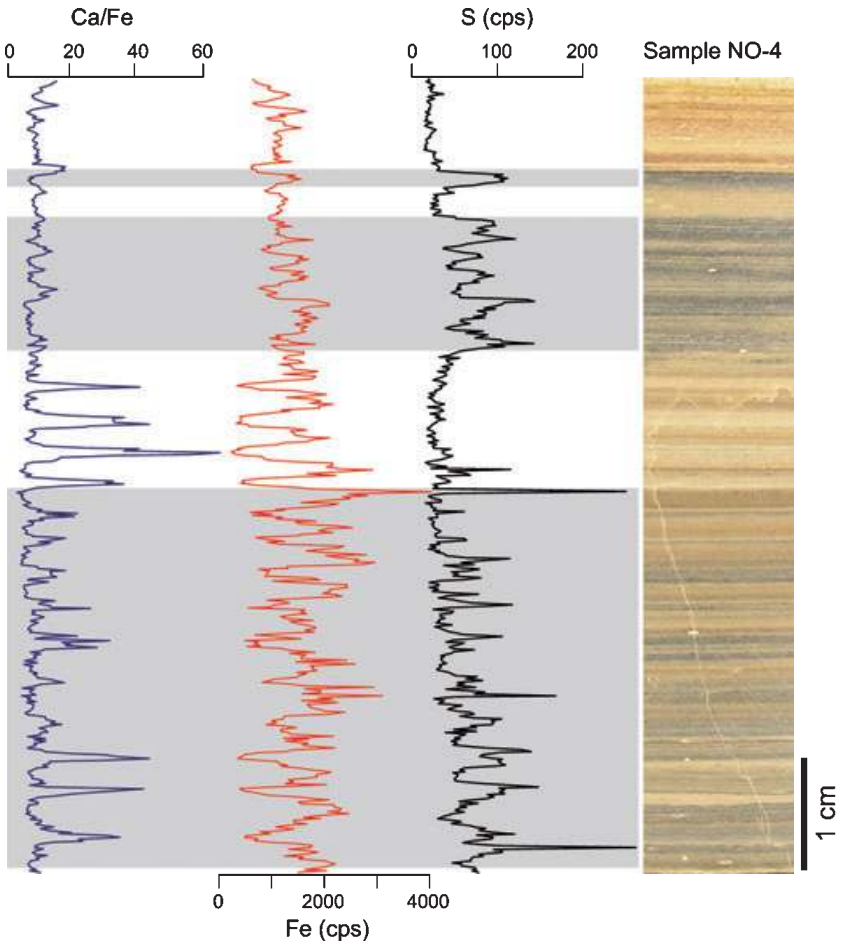

Fig. 6. Ultra high-resolution μ-XRF scanning of a 7 cm slab of LL facies of the Nova Olinda Member (Nova Olinda quarry). Ca/Fe ratio, Fe and S intensities (in counts per second, cps) are shown. μ-XRF results are plotted versus slab height; grey bands correspond to visually darker horizons.

porosity, and the loose packing of the well-developed calcite rhombohedra attest to only minor compaction and limited cementation (Fig. 4A to D). In contrast, the clay-poor LL facies shows a higher degree of cementation, accompanied by a significant reduction of interparticle porosity between individual calcite crystals (Fig. 4E and F).

According to Wright *et al.* (1997), the development of a microporous crystal framework in Miocene lacustrine chalks may reflect extensive recrystallization, resulting in a porous framework of subhedral to euhedral crystals (with grain size ranging from *ca* 0·5 to 3 μm). However, given the significant differences in ultrastructure (including grain size and shape), a purely replacive origin of the crystal framework in the Nova Olinda laminites is considered unlikely. Alternatively, the preservation of the original texture and mineralogy in microporous mudstones has been related to the inhibition of cementation in closed diagenetic systems with high rock/water ratios and the absence of an external carbonate source (Moshier, 1989). Reduced compaction and retention of primary depositional porosity has been observed in overpressured chalks during burial diagenesis (Maliva & Dickson, 1992). In addition, the occurrence of clay coatings on crystal surfaces can act as an effective inhibitor for the chemical bonding of calcite, resulting in limited cementation (Tucker & Wright, 1990). In a case study on Palaeogene lacustrine chalky carbonates from the Madrid Basin, Arribas *et al.* (2004) were able to show that the preservation of the primary textural and compositional inventory was controlled mainly by: (i) the stable mineralogy of the primary carbonate mud; (ii) an early authigenesis of clay minerals; and (iii) retention of an Mg-enriched fluid in the overpressured pore system. Similar processes may have acted on the chalky Nova Olinda carbonates, preventing extensive cementation and recrystallization. Here, the overlying and underlying fine-grained siliciclastics (Batateiras

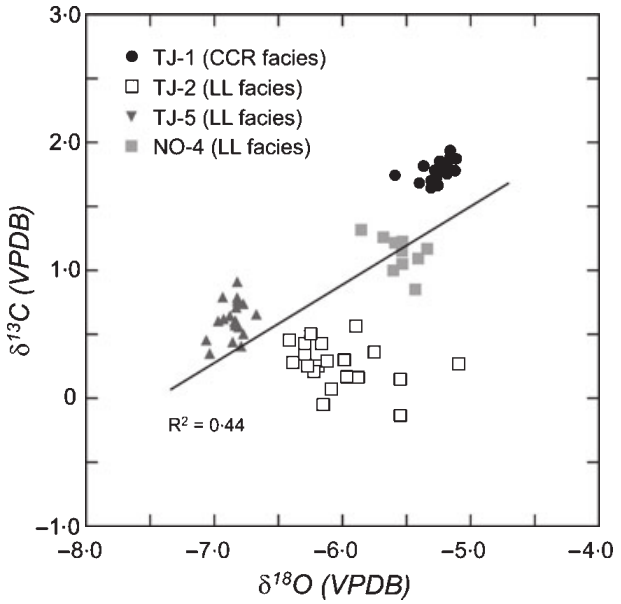

Fig. 7. Cross-plot of all measured stable-isotope data from the Nova Olinda Member showing distinct clustering of values from individual slabs. An all-over positive covariance (R^2 = 0·44) reflects depletion of both δ^{13}C and δ^{18}O with increasing water depth, and is considered typical for hydrologically closed lake basins (Talbot, 1990). Refer to Fig. 3 for the position of the individual samples.

Formation and Caldas Member, respectively) may have acted as an effective permeability barrier, resulting in compartmentalization of the chalky carbonates and in reduced fluid flow. The distinct differences in cement growth and pore-space reduction observed between CCR and LL facies may reflect primary lithological differences in clay mineral content.

Origin of the carbonate

In lacustrine environments, possible sources for the carbonate fraction include: (i) clastic input derived from allochthonous carbonates; (ii) biogenic hardparts, calcareous skeletons and benthonic microbial precipitates; and (iii) biologically induced and/or mediated precipitation of autochthonous carbonate minerals.

The sedimentary record of the Nova Olinda Member does not provide evidence for a significant contribution of clastic carbonate detritus to the basin, either from erosion of nearby outcropping limestone terrain or from reworking of littoral sediments. Sedimentary features like mass-wasting deposits, graded bedding or debris flows, indicating transport of allochthonous material to the basin, are virtually absent. An exception is represented by a single debris flow layer (*ca* 0·75 m thick) associated with extensive slumping which crops out in the vicinity of Tatajuba (Heimhofer & Martill, 2007). As demonstrated by Fuersich *et al.* (2007), fine-grained, allochthonous, re-deposited material can represent a significant proportion of the carbonate in laminated plattenkalk facies. However, field sedimentological and thin-section analyses of the Nova Olinda laminites do not show any small-scale grading or erosive contacts indicative of deposition from high-density currents or suspension settling. The absence of detrital dolomite particles and the well-preserved angular shape of the calcite crystals contradict substantial erosion, transport and re-deposition (Kelts & Hsü, 1978) and support instead an autochthonous origin. Furthermore, there is no indication of significant input from bioclastic carbonate particles, either on the macroscopic or microscopic scale. Apart from the sporadic occurrence of calcareous ostracod carapaces, the quantitative contribution of bioclastic carbonate is considered to be negligible.

Certain sedimentary structures within the Nova Olinda Member have been interpreted to reflect *in situ* precipitation and/or trapping and binding of carbonate particles by a microbial mat community thriving at the bottom of the basin. Based on the rare occurrence of low-amplitude ripple-like textures and creased layers, Martill & Wilby (1993) speculate about the occurrence of benthonic microbial mats or biofilms. Further evidence is derived from the upper LL unit (Jamacaru Member) which is characterized by partially silicified and brecciated dome-shaped bodies that resemble a stromatolite layer (Martill *et al.*, 2007b). Similarly, rhythmically laminated carbonate–siliciclastic couplets with abundant pellets, microbialites and fibrous organic matter have been reported from the lacustrine deposits of the Oligocene Creede Formation. Here, a resemblance to phototrophic bacterial mats has been proposed based on the patchiness and stringiness of individual organic laminae as well as on the occurrence of multiple sub-laminations with calcium carbonate (Finkelstein *et al.*, 1999). However, the bulk of the Nova Olinda laminites lack the sedimentary inventory of typical benthonic microbial-derived microbialites. Widespread wrinkle lamination or characteristic build-up geometries are absent and the extraordinarily fine and regular bedding, as well as the lateral continuity of individual laminae, rather points to a passive sedimentation process. This observation is supported by ultrastructure analysis, which

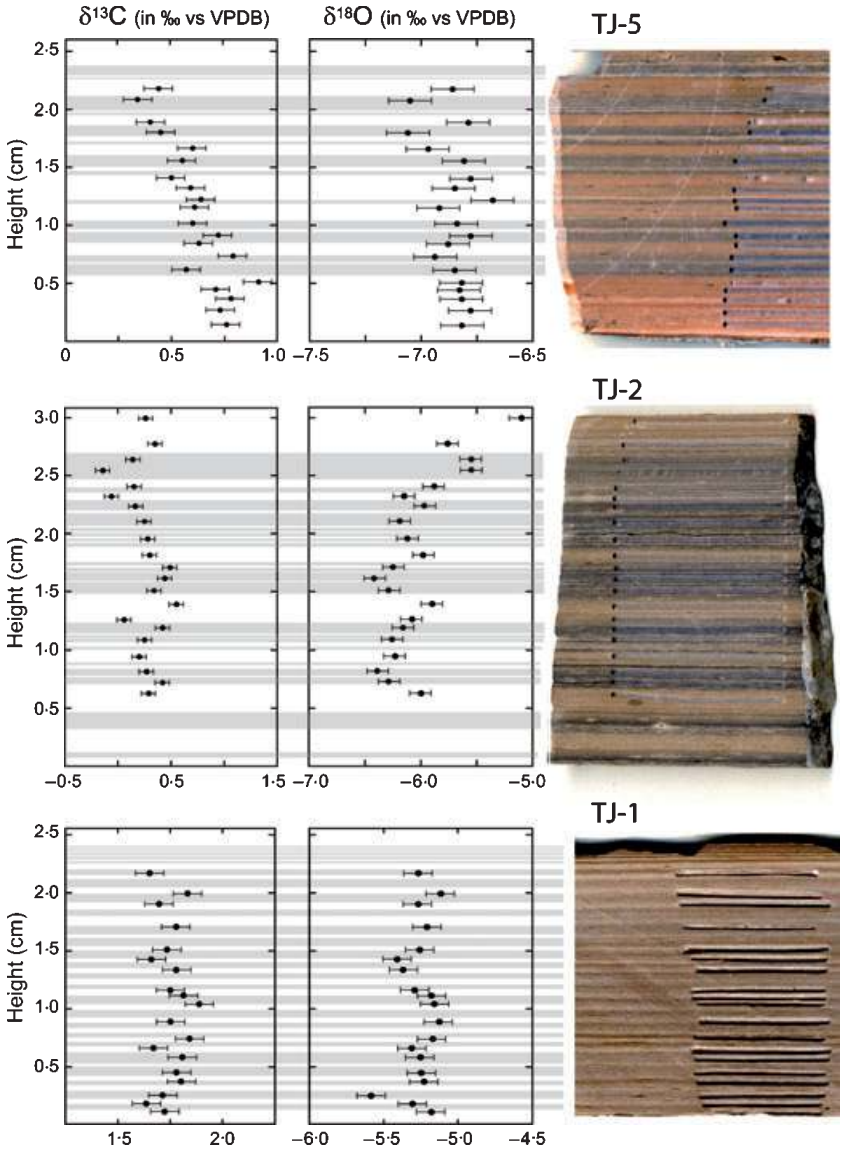

Fig. 8. High-resolution stable carbon and oxygen isotope results from three sample slabs, Tatajuba quarry. Sample TJ-1 corresponds to CCR facies; TJ-2 and TJ-5 represent LL facies. Individual laminae were sampled parallel to bedding using a Merchantek MicroMill device. Grey bars correspond to dark laminae visible on the corresponding slab. All stable-isotope values are reported in per mil versus VPDB. See Fig. 3 for location of individual samples.

provides no evidence for typical microbial-derived crystal shapes including, for example, the commonly described microspheroids, dumbbells, peloids, peloid-like allochems, fan-like crystals or calcified filaments (Freytet & Verrecchia, 1998; Tribovillard, 1998; Folk & Chafetz, 2000; Duque-Botero & Maurrasse, 2008). The idiomorphic crystal shape, crystal size, the homogenous grain-size distribution and the apparent lack of intergrowth between the individual calcite crystals contradicts *in situ* growth of the rhombohedra and polyhedra and rather supports biologically induced and/or mediated precipitation from the water column.

In modern lakes, the authigenic precipitation of carbonate minerals (so-called 'whitings') is a widely observed process, which accounts for the bulk of the primary carbonate in many hard-water lakes (Kelts & Hsü, 1978; Stabel, 1986; Anderson & Dean, 1988; Teranes *et al.*, 1999). Temperature increase in the upper water layer (for example, during the seasonal cycle) results in decreased $CaCO_3$ solubility. This process is often associated with phytoplankton and picoplankton blooms, causing chemical disequilibrium by abstracting large volumes of CO_2 from surface waters. As demonstrated by Thompson *et al.* (1997), phototrophic picoplankton can act as a small,

biologically active nucleation site for the growth of calcite crystals. The combination of seasonally fluctuating phytoplankton and picoplankton activity and temperature increase initiates the precipitation of calcite crystals in the upper water column which settle and accumulate at the bottom.

This type of biologically induced and/or mediated precipitation process has been reported from many modern temperate and high-latitude settings (Kelts & Hsü, 1978; Hollander *et al.*, 1992; Lotter *et al.*, 1997; Teranes *et al.*, 1999). In mid-latitude and tropical lakes, phytoplankton and picoplankton growth may be stimulated by annual lake water mixing and increased nutrient availability resulting in seasonality-driven carbonate precipitation (Thompson *et al.*, 1997; Lamb *et al.*, 2002; Leng & Marshall, 2004). Authigenic precipitation of calcite has also been suggested for a number of fossil freshwater carbonates, including, for example, the Orcadian Basin (Devonian, UK; Janaway & Parnell, 1989; Stephenson *et al.*, 2006), the Slawkow Graben (Permian, Poland; Szulc & Cwizewicz, 1989), the Krkonoše Piedmont Basin (Permian, Czech Republic; Martinek *et al.*, 2006), the La Serranía de Cuenca Basin (Early Cretaceous, Spain; Gómez Fernández & Meléndez, 1991) and the Madrid Basin (Palaeogene, Spain; Arribas *et al.*, 2004).

Depositional environment

Deposition of the Nova Olinda limestone took place under very quiet and protected conditions, as evidenced by the persistent occurrence of an undisturbed and continuous lamination pattern. The absence of any sedimentary structures indicating turbulence or current activity points towards deposition below storm wave base and a low sub-aquatic relief (Heimhofer & Martill, 2007). Conditions in the lower part of the water body were unfavourable for bottom-dwelling organisms as indicated by the complete lack of a benthonic assemblage, bioturbation structures or other trace fossils (Martill & Wilby, 1993). Based on faunal considerations, Mabesoone & Tinoco (1973) as well as Maisey (1991) proposed deposition of the Nova Olinda Member under freshwater conditions. This interpretation has been challenged by findings of hopper-faced halite pseudomorphs (partly with marcasite overgrowth) in several horizons of the Nova Olinda Member, which attest to the episodic development of hypersaline conditions in bottom waters, at least during certain episodes (Martill & Wilby, 1993; Martill *et al.*, 2007b). To explain the contrasting evidence, Martill & Wilby (1993) favoured a stratified water body with hypersaline bottom waters overlain by tongues of freshwater. In such a scenario, dissolution of pre-existing evaporites may account for the high salinities and precipitation of halite at the sediment surface or within the sediment. Hydrochemical degradation of lake waters and the establishment of hypersaline conditions due to the dissolution of pre-existing salt deposits is a phenomenon observed in modern lacustrine environments (Gutiérrez *et al.*, 2008).

According to Neumann *et al.* (2003), the deposition of the Crato lacustrine sequence was affected by alternating humid-arid cycles resulting in significant lake-level fluctuations. However, based on the existing evidence, a tectonic control on lake-level evolution as proposed, for example, for the nearby Codó Formation of the Grajaú Basin cannot be ruled out (Paz & Rossetti, 2006). In the idealized lacustrine parasequence of Neumann *et al.* (2003) (*sensu* Carroll & Bohacs, 1999), lowstand deposits are represented by deltaic siliciclastics, which are overlain by mudstones, oil shales and mixed siliciclastic–carbonate facies reflecting deepening of the water body during the transgressive phase. Deposition of laminated carbonate facies took place during episodes of lake-level highstand and was restricted to basinal or off-shore zones, far away from the influence of marginal facies belts. Following the interpretation of Neumann *et al.* (2003), CCR facies correspond to the early and late phase of lake-level highstand. In contrast, the relatively pure limestones of the LL facies occur in the most distal part of the lacustrine setting and reflect deposition during maximum highstand.

High-resolution μ-XRF results of both types of laminated facies indicate a low contribution of catchment-derived siliciclastic material to the basin during highstand. Intensities of elements typically associated with allochthonous sources (e.g. Al, K, Ti and Si) are particularly low, highlighting limited catchment input of siliciclastics. Only Fe represents an exception to this rule. The general pattern accords well with the absence of a significant clastic fraction as confirmed in thin-section and under the SEM. Trapping of the detrital allochthonous component in the more proximal facies belts during highstand conditions may account for the reduced input of catchment-derived siliciclastic material, at least to a certain extent. According to Gierlowski-Kordesch (1998), thick, basinwide, non-marine

carbonate deposits must be connected to a carbonate-rich source area; reduced clastic input alone cannot account for their formation. Hence, substantial input of Ca and HCO_3^- ions is proposed, reflecting the drainage and weathering of carbonate-rich rocks in the watershed. For the Nova Olinda Member, sedimentological and petrographic results point towards the dominance of authigenic carbonate precipitation throughout the basin. Thus, fluctuations in the Ca/Fe ratio can be considered as indicative of a variable input of allochthonous and autochthonous material. Fe-bearing rocks and soils from the catchment area may be the source of this element, and the changing input to the basin may be related to concomitant changes in environmental conditions. The Fe/Mn ratio closely follows variations in allochthonous input that may indicate low diagenetic imprint because Mn enrichment usually accompanies early diagenetic processes commonly taking place along the Fe(II)/Fe(III) redox boundary (Schaller *et al.*, 1997).

In the CCR facies, a strong covariance of Fe and S intensities, in combination with the clear correspondence between S intensities and the visually distinct dark-grey colour pattern, points to pyrite as the main S-bearing mineral phase (Fig. 5); this is in accordance with the microscopically observed enrichment of finely disseminated pyrite within the dark-grey layers. Pyrite formation is usually attributed to bacterial sulphate reduction, an important process for the degradation of organic matter under anaerobic conditions (Berner, 1985). In the CCR facies, high pyrite contents within dark laminae are accompanied by increased organic matter, thus giving support to the above-mentioned process. In marked contrast, S and Fe intensities are more or less decoupled in the LL facies (Fig. 6). Here, only S displays a clear correspondence with dark-grey colouring and pyrite enrichment, whereas peaks in Fe correlate well with dark-brown laminae devoid of organic matter. In these intervals, enhanced input of Fe did not stimulate an increase in productivity followed by pyrite formation, probably because of the lack of other biolimiting nutrients or increased salinities in the more distal parts of the basin.

Watershed palaeohydrology and palaeolimnology

Thermal and/or salinity-driven stratification and the occurrence of a chemocline separating stagnant bottom waters from an overlying freshwater layer has already been proposed for the Crato Basin, based on palaeontological and sedimentological evidence (Martill *et al.*, 2007b). Such a scenario is in good agreement with the new geochemical findings. The $\delta^{18}O$ composition of all measured samples ranges between about −5‰ and −7‰ and therefore differs significantly from late Early Cretaceous marine signatures. Time-equivalent values derived from Late Aptian marine sea surface waters fluctuate between −0·5‰ and −1·5‰ at low latitudes (Mazagan Plateau, Herrle, 2002) and between −1·0 and 0‰ at higher latitudes (Falkland Plateau; Clarke & Jenkyns, 1999). Hence, the consistent negative $\delta^{18}O$ signature of the authigenic calcite points to precipitation from a ^{18}O-poor meteoric source and confirms a lacustrine/non-marine environment for the Nova Olinda Member. Similar negative oxygen isotope values have been used to identify continental freshwater settings throughout the geological record (Janaway & Parnell, 1989; Camoin *et al.*, 1997; Martinek *et al.*, 2006; Paz & Rossetti, 2006).

Compared with many modern and fossil lacustrine settings (Talbot, 1990; Paz & Rossetti, 2006; Bowen *et al.*, 2008), the freshwater layer of the Nova Olinda Member was characterized by relatively positive $\delta^{13}C$ values (−0·2 to 1·9‰). This carbon isotopic signature is in accordance with a scenario invoking stagnant and oxygen-deficient bottom waters, as indicated by the lamination pattern and exceptional fossil preservation of the Crato beds (Martill *et al.*, 2007a). Biological productivity in concert with water column stratification can have a significant impact on the $\delta^{13}C$ of the dissolved inorganic carbon (DIC) in lacustrine settings. Preferred uptake of ^{12}C by aquatic photoautotrophic organisms will lead to depletion of the surface water carbon pool. At the same time, stratification and reduced mixing prevents replenishment of surface waters with ^{12}C-rich carbon, resulting in higher $\delta^{13}C$ values of the DIC and, in consequence, of authigenic precipitates (McKenzie, 1985; Leng & Marshall, 2004). Alternatively, isotopic equilibration with atmospheric CO_2 may have caused the relatively high $\delta^{13}C$ values observed in the Crato laminites. Many modern large closed basin lakes, especially in low-latitude regions, are characterized by $\delta^{13}C$ values ranging between +1‰ and +3‰, for example, the large African rift basin lakes of Turkana or Malawi (Ricketts & Johnson, 1996). Finally, the dissolution of pre-existing marine limestones in the catchment area may also have had an effect on the carbon isotopic composition of the inflowing

water and could account, at least to a certain extent, for the positive $\delta^{13}C$ values (Andrews *et al.*, 1997).

Cyclic changes in primary productivity as reported for Holocene sediments in modern temperate lakes (McKenzie, 1982; Teranes *et al.*, 1999) are, however, not evident in the stable isotope records of the Crato laminites. The high-resolution dataset from Tatajuba does not show the expected cyclical changes in the stable isotopic composition associated with changes in colour pattern, neither for LL nor for CCR facies. Despite the good preservation of primary fabrics, partial or complete homogenization of the original stable isotopic signatures during diagenesis cannot be ruled out. The formation of secondary calcite spar between idiomorphic rhombohedra has been documented clearly for LL facies and probably affects the stable isotopic composition of the bulk carbonate to a certain extent. In addition, neomorphic processes, including epitaxial overgrowth of crystals or fabric-preserving replacement of the primary mineralogy, could affect the stable isotopic signal and may account for the relatively uniform compositions (Tucker & Wright, 1990; Wright *et al.*, 1997). On the other hand, the absence of a cyclic signal in the isotopic record may be explained by environmental factors. Permanent stratification could have prevented the seasonal turn-over of the system and thus limited the input of ^{12}C-rich waters to the mixolimnion. Absence of seasonal mixing would also be consistent with the palaeolatitude of the Crato Basin close to the equator (Hay *et al.*, 1999).

Despite the lack of short-term variability on the laminae-scale, overall stratigraphic trends in the stable isotopic data from Tatajuba can be associated with palaeoenvironmental changes. Finely laminated and clay-rich CCR facies, which correspond to the early phase of lake-level highstand (Neumann *et al.*, 2003), are characterized by the most positive $\delta^{13}C$ values and the least negative $\delta^{18}O$ values. During this phase, the water body of the lake was influenced by rising water level but throughflow most probably was limited. Increased residence time of water in a restricted basin would have promoted equilibration with atmospheric CO_2, probably accompanied by stagnant conditions and low input from plant-derived and soil-derived CO_2. During maximum highstand, as reflected by the deposition of more distal, siliciclastic-poor LL facies, the basin was characterized by more open hydrological conditions. Enhanced throughflow and reduced evaporation may be reflected in the $\delta^{18}O$ signal, which shows a shift of *ca* 2‰ towards more negative values with increasing water depth. In such a scenario, lake-level highstand would have been accompanied by a shift in precipitation/evaporation ratio, causing increased runoff during a more humid climate. Alternatively, the observed trend in $\delta^{18}O$ could reflect changes in lake water temperature. However, given the almost equatorial position of the basin during the Early Cretaceous, only minor variations in mean annual temperatures are expected, which were probably insufficient to account for the observed shifts.

In closed and semi-closed basin lakes, factors controlling the $\delta^{13}C$ and $\delta^{18}O$ composition are commonly coupled, resulting in covariance of the two isotope systems; this is attributed conventionally to the residence time of water in the lake system or, on shorter time scales, to changes in seasonal climate patterns (Talbot, 1990; Drummond *et al.*, 1995; Li & Ku, 1997). An all-over positive covariance of the composite dataset between C and O isotope ratios ($R^2 = 0{\cdot}44$) from the laminites is interpreted to reflect the temporal evolution of water and DIC isotopic compositions and indicates that deposition took place in a hydrologically closed or semi-closed water body, at least during the onset of carbonate laminite formation. Compared with Holocene records from closed basin lakes, the correlation for the Crato Formation is rather weak (Talbot, 1990; Drummond *et al.*, 1995); this may in part reflect the transition from a closed or semi-closed to a hydrologically more open lake system. As pointed out by Bowen *et al.* (2008), the strongest isotopic covariance is usually observed during short intervals of significant lake-volume changes, typically associated with Holocene climate change. Hence, the absence of a strong isotopic covariance may also reflect the discontinuous sampling and the relatively coarse resolution of the outcrop samples.

CONCLUSIONS

The laminated facies of the Crato fossil beds of the Araripe Basin in North-eastern Brazil provide one of the best preserved lacustrine sedimentary records for the Mesozoic of Gondwana. This multiproxy study of the laminites of the Nova Olinda Member represents an attempt to constrain the palaeoenvironmental conditions of deposition. Combining high-resolution sedimentological and geochemical datasets, the following main conclusions can be drawn:

1 The bulk of the carbonate fine-fraction originates from authigenic precipitation within the epilimnion, most probably induced and/or mediated by biochemical processes. Clear evidence for a significant carbonate contribution from a benthonic microbial community is lacking.

2 The development of a stratified anoxic and/or hypersaline water column allowed the preservation of an undisturbed lamination pattern composed of organic/pyrite-rich dark and carbonate-rich light laminae. Ultra-high resolution elemental analyses using μ-XRF scanning indicate limited but variable allochthonous input into the basin that is visually reflected by variations in colour and thickness of individual laminae.

3 The C and O stable isotopic composition of the authigenic carbonate fraction confirms a lacustrine origin; their co-variance further indicates the closed or semi-closed basin nature of the system. The C isotopic signature may indicate equilibration with atmospheric CO_2, probably accompanied by enhanced water column stratification and low input of plant or soil derived carbon. At the current stage, the absence of a cyclic stable isotope pattern in concert with the prominent lamination remains ambiguous; homogenization of the signal during diagenesis cannot be ruled out.

ACKNOWLEDGEMENTS

We thank Ulrike Schulte, Dieter Buhl and Rolf Neuser for laboratory assistance and Robert Loveridge (University of Portsmouth) for his support during field work in Brazil. Furthermore, we would like to thank Elizabeth Gierlowski-Kordesch and an anonymous reviewer who greatly improved the manuscript. Financial support from DFG project HE 4467/1-1 and by the NRW Akademie der Wissenschaften to UH is gratefully acknowledged.

REFERENCES

Anderson, R.Y. and **Dean, W.E.** (1988) Lacustrine varve formation through time. *Palaeogeogr. Palaeoclimatol. Palaeoecol.*, **62,** 215–235.

Andrews, J.E., Riding, J.B. and **Dennis, P.F.** (1997) The stable isotope record of environmental and climatic signals in modern terrestrial microbial carbonates from Europe. *Palaeogeogr. Palaeoclimatol. Palaeoecol.*, **129,** 171–189.

Arai, M. (2000) Chapadas: relicts of mid-Cretaceous interior seas in Brazils. *Rev. Bras. Geosci.*, **30,** 436–438.

Arribas, M.E., Bustillo, A. and **Tsige, M.** (2004) Lacustrine chalky carbonates: origin, physical properties and diagenesis (Palaeogene of the Madrid Basin, Spain). *Sed. Geol.*, **166,** 335–351.

Batten, D.J. (2007) Spores and pollen from the Crato Formation: biostratigraphic and palaeoenvironmental implications. In: *The Crato Fossil Beds of Brazil – Window into an Ancient World* (Eds D.M. Martill, G. Bechly and R.F. Loveridge), pp. 566–573. Cambridge University Press, Cambridge.

Baudin, F. and **Berthou, P.-Y.** (1996) Depositional environments of the organic matter of Aptian-Albian sediments from the Araripe Basin (NE Brazil). *Bull. Centres Rech. Explor.-Prod. Elf-Aquitaine*, **20,** 213–227.

Berner, R.A. (1985) Sulfate reduction, organic-matter decomposition and pyrite formation. *Philos. Trans. R Soc.*, **315,** 25–38.

Berthou, P.-Y., Viana, M. and **Campos, D.** (1990). Coupe de la Formation Santana dans le secteur de ''Pedra Branca'' (Santana do Cariri) (Bassin d'Araripe, NE du Brésil). In: *Contribution à l'étude de la sédimentologie et des paléoenvironnements* (Eds D. Campos, M. Viana, P. Brito and G. Beurlen), pp. 173–191. Atas do I Simposio sobre a Bacia do Araripe e Bacias Interiores do Nordeste, Crato, Ceara, Brazil.

Bowen, G.J., Daniels, A.L. and **Bowen, B.B.** (2008) Paleoenvironmental isotope geochemistry and paragenesis of lacustrine and palustrine carbonates, Flagstaff Formation, central Utah, USA. *J. Sed. Res.*, **78,** 162–174.

Camoin, G., Casanova, J., Rouchy, J.M., BlancValleron, M.M. and **Deconinck, J.F.** (1997) Environmental controls on perennial and ephemeral carbonate lakes: the central palaeo-Andean Basin of Bolivia during Late Cretaceous to early Tertiary times. *Sed. Geol.*, **113,** 1–26.

Carroll, A.R. and **Bohacs, K.M.** (1999) Stratigraphic classification of ancient lakes: balancing tectonic and climatic controls. *Geology*, **27,** 99–102.

Cavalcanti, V. and **Vianna, M.** (1990). Faciologica dos sedimentos não-lacustres da Formação Santana (Cretáceo Inferior da Bacia do Araripe, nordeste do Brasil). In: *Atas do I Simposio Sobre Bacia do Araripe e Bacias Interiores do Nordeste* (Eds D. Campos, C.F. Viana, P.M. Brito and G. Beurlen), 405 pp. D.N.P.M, Crato, Ceara, Brazil.

Chang, H.K., Kowsmann, R.O. and **de Figueiredo, A.M.F.** (1988) New concepts on the development of East Brazilian Marginal Basins. *Episodes*, **11,** 194–202.

Chumakov, N.M., Zharkov, M.A., Herman, A.B., Doludenko, M.P., Kalandadze, N.M., Lebedev, E.L., Ponomarenko, A.G. and **Rautian, A.S.** (1995) Climatic belts of the mid-Cretaceous time. *Stratigr. Geol. Correl.*, **3,** 241–260.

Clarke, L.J. and **Jenkyns, H.C.** (1999) New oxygen isotope evidence for long-term Cretaceous climate change in the Southern Hemisphere. *Geology*, **27,** 699–702.

Coimbra, J.C., Arai, M. and **Carreno, A.L.** (2002) Biostratigraphy of Lower Cretaceous microfossils from the Araripe Basin, northeastern Brazil. *Géobios*, **35,** 687–698.

Doyle, J.A., Jardiné, S. and **Doerenkamp, A.** (1982) *Afropollis*, a new genus of early angiosperm pollen, with notes on the Cretaceous palynostratigraphy and palaeoenvironments of northern Gondwana. *Bull. Centres Rech. Explor.-Prod. Elf-Aquitaine*, **6,** 39–117.

Drummond, C.N., Patterson, W.P. and **Walker, J.C.G.** (1995) Climatic forcing of carbon–oxygen isotopic covariance in temperate-region marl lakes. *Geology*, **23,** 1031–1034.

Duque-Botero, F. and **Maurrasse, F.** (2008) Role of cyanobacteria in Corg-rich deposits: an example from the Indidura

Formation (Cenomanian–Turonian), northeastern Mexico. *Cretaceous Res.*, **29,** 957–964.

Finkelstein, D.B., Hay, R.L. and **Altaner, S.P.** (1999) Origin and diagenesis of lacustrine sediments, upper Oligocene Creede Formation, southwestern Colorado. *Geol. Soc. Am. Bull.*, **111,** 1175–1191.

Folk, R.L. (1959) Practical petrographic classification of limestones. *AAPG Bull.*, **43,** 1–38.

Folk, R.L. and **Chafetz, H.S.** (2000) Bacterially induced microscale and nanoscale carbonate precipitates. In: *Microbial Sediments* (Eds R.B. Riding and S.M. Awramik), pp. 40–49. Springer Verlag, Berlin, Germany.

Franzen, J.L. and **Michaelis, W.** (1988) Eocene Lake Messel. *Courier Forschungsinstitut Senckenberg*, **107,** 1–452.

Fregenal-Martínez, M.A. and **Meléndez, N.** (1994) Sedimentological analysis of the Lower Cretaceous lithographic limestones of the La Hoyas fossil site (Serranía de Cuenca, Iberian Range, Spain. *Geobios. Mem. Spec.*, **16,** 185–193.

Freytet, P. and **Verrecchia, E.P.** (1998) Freshwater organisms that build stromatolites: a synopsis of biocrystallization by prokaryotic and eukaryotic algae. *Sedimentology*, **45,** 535–563.

Fuersich, T., Werner, W., Schneider, S. and **Mauser, M.** (2007) Sedimentology, taphonomy, and palaeoecology of a laminated plattenkalk from the Kimmeridgian of the northern Franconian Alb (southern Germany). *Palaeogeogr. Palaeoclimatol. Palaeoecol.*, **243,** 92–117.

Gardner, G. (1846) *Travels in the Interior of Brazil, Principally through the Northern Province and the Gold and Diamond Districts during the Years 1836–1841.* Reeves Brothers, London.

Gierlowski-Kordesch, E.H. (1998) Carbonate deposition in an ephemeral siliciclastic alluvial plain: Jurassic Shuttle Meadow Formation, Hartford Basin, Newark Supergroup, USA. *Palaeogeogr. Palaeoclimatol. Palaeoecol.*, **140,** 161–184.

Gómez Fernández, J.C. and **Meléndez, N.** (1991) Rhythmically laminated lacustrine carbonates in the Lower Cretaceous of La Serranía de Cuenca Basin (Iberian Ranges, Spain). *Spec. Publ. Int. Assoc. Sedimentol.*, **13,** 245–256.

Gutiérrez, F., Calaforra, J.M., Cardona, F., Ortí, F., Durán, J.J. and **Garay, P.** (2008) Geological and environmental implications of the evaporite karst in Spain. *Environ. Geol.*, **53,** 951–965.

Hay, W.W., DeConto, R.M., Wold, C.N., Wilson, K.M., Voigt, S., Schulz, M., Wold, A.R., Dullo, W.C., Ronov, A.B., Balukhovsky, A.N. and **Soeding, E.** (1999). Alternative global Cretaceous paleogeography. In: *Evolution of the Cretaceous Ocean-Climate System*, Vol. 332, pp. 1–47. Geol Soc Am, Boulder.

Heimhofer, U. and **Martill, D.M.** (2007) The sedimentology and depositional environment of the Crato Formation. In: *The Crato Fossil Beds of Brazil – Window into an Ancient World* (Eds D.M. Martill, G. Bechly and R.F. Loveridge), pp. 44–62. Cambridge University Press, Cambridge.

Herrle, J.O. (2002). *Paleoceanographic and Paleoclimatic Implications on mid-Cretaceous Black Shale Formation in the Vocontian Basin and the Atlantic: Evidence from Calcareous Nannofossils and Stable Isotopes.* Universität Tübingen, Tübingen, 115 pp.

Hollander, D.J., McKenzie, J.A. and **Lotenhaven, H.** (1992) A 200-year sedimentary record of progressive eutrophication in Lake Greifen (Switzerland) – implications for the origin of organic-carbon-rich sediments. *Geology*, **20,** 825–828.

Janaway, T.M. and **Parnell, J.** (1989) Carbonate production within the Orcadian Basin, northern Scotland – a petrographic and geochemical study. *Palaeogeogr. Palaeoclimatol. Palaeoecol.*, **70,** 89–105.

Kelts, K. and **Hsü, K.J.** (1978) Freshwater carbonate sedimentation. In: *Lakes – Chemistry, Geology, Physics* (Ed. A. Lerman), pp. 295–323. Springer, Berlin/Heidelberg.

Lamb, A.L., Leng, M.J., Lamb, H.F., Telford, R.J. and **Mohammed, M.U.** (2002) Climatic and non-climatic effects on the $\delta^{18}O$ and $\delta^{13}C$ compositions of Lake Awassa, Ethiopia, during the last 6.5 ka. *Quatern. Sci. Rev.*, **21,** 2199–2211.

Last, W.M. (1992) Petrology of modern carbonate hardgrounds from East Basin Lake, a saline maar lake, southern Australia. *Sed. Geol.*, **81,** 215–229.

Leng, M.J. and **Marshall, J.D.** (2004) Palaeoclimate interpretation of stable isotope data from lake sediment archives. *Quatern. Sci. Rev.*, **23,** 811–831.

Li, H.-C. and **Ku, T.-L.** (1997) $\delta^{13}C$–$\delta^{18}O$ covariance as a paleohydrological indicator for closed-basin lakes. *Palaeogeogr. Palaeoclimatol. Palaeoecol.*, **133,** 69–80.

Lotter, A.F., Sturm, M., Teranes, J.L. and **Wehrli, B.** (1997) Varve formation since 1885 and high-resolution varve analyses in hypertrophic Baldeggersee (Switzerland). *Aquat. Sci.*, **59,** 304–325.

Mabesoone, J.M. and **Tinoco, I.M.** (1973) Palaeoecology of the aptian santana formation (Northeastern Brazil). *Palaeogeogr. Palaeoclimatol. Palaeoecol.*, **14,** 97–118.

Maisey, J.G. (1991). *Santana Fossils: An illustrated Atlas.* Tropical Fish Hobbyist Publications, New Jersey, 459 pp.

Maliva, R.G. and **Dickson, J.A.D.** (1992) Microfacies and diagenetic controls of porosity in Cretaceous/Tertiary chalks, Eldfisk Field, Norwegian North Sea. *AAPG Bull.*, **76,** 1825–1838.

Martill, D.M. and **Davis, P.G.** (2001) A feather with possible ectoparasite eggs from the Crato Formation (Lower Cretaceous, Aptian) of Brazil. *Neues. Jahrb. Geol Palaeontol. Abh*, **219,** 241–259.

Martill, D.M. and **Frey, E.** (1995) Colour patterning preserved in Lower Cretaceous birds and insects: the Crato Formation of N.E. Brazil. *Neues Jahrbuch fuer Geologie und Palaeontologie Monatshefte* **2,** 118–128.

Martill, D.M. and **Heimhofer, U.** (2007) Stratigraphy of the Crato Formation. In: *The Crato Fossil Beds of Brazil – Window into an Ancient World* (Eds D.M. Martill, G. Bechly and R.F. Loveridge), pp. 25–43. Cambridge University Press, Cambridge.

Martill, D.M. and **Wilby, P.** (1993) Stratigraphy. In: *Fossils of the Santana and Crato Formations, Brazil* (Ed. D.M. Martill), pp. 20–50. The Palaeontological Association, London.

Martill, D.M., Bechly, G. and **Loveridge, R.** (2007a). *The Crato Fossil Beds of Brazil – Window into an Ancient World.* Cambridge University Press, Cambridge, 625 pp.

Martill, D.M., Loveridge, R.F. and **Heimhofer, U.** (2007b) Halite pseudomorphs in the Crato Formation (Early Cretaceous, Late Aptian-Early Albian), Araripe Basin, Northeast Brazil: further evidence for hypersalinity. *Cretaceous Res.*, **28,** 613–620.

Martill, D.M., Loveridge, R.F. and **Heimhofer, U.** (2008) Dolomite pipes in the Crato formation fossil lagerstätte (Lower Cretaceous, Aptian), of northeastern Brazil. *Cretaceous Res.*, **29,** 78–86.

Martinek, K., Blecha, M., Danek, V., Francu, J., Hladikova, J., Johnova, R. and **Ulicny, D.** (2006) Record of palaeoenvironmental changes in a Lower Permian organic-rich lacustrine succession: integrated sedimentological and geochemical study of the Rudnik member, Krkonose

Piedmont Basin, Czech Republic. *Palaeogeogr. Palaeoclimatol. Palaeoecol.*, **230,** 85–128.

de Matos, R.M.D. (1999). History of the northeast Brazilian rift system: kinematic implications for the break-up between Brazil and West Africa. In: *The Oil and Gas Habitats of the South Atlantic* (Eds N.R. Cameron, R.H. Bate and V.S. Clure), *Geol. Soc. Lond. Spec. Publ.*, Vol. 153, pp. 55–73. Geological Society, London.

McKenzie, J. (1982) Carbon-13 cycle in Lake Greifen: a model for restricted ocean basins. In: *Nature and Origin of Cretaceous Carbon-Rich Facies* (Eds S.O. Schlanger and M.B. Cita), pp. 197–207. Academic Press, London.

McKenzie, J.A. (1985) Carbon isotopes and productivity in the lacustrine and marine environment. In: *Chemical Processes in Lakes* (Ed. W. Stumm). Wiley, New York, pp. 99–118.

Menon, F. and **Martill, D.M.** (2007) Taphonomy and preservation of Crato Formation arthropods. In: *The Crato Fossil Beds of Brazil – Window into an Ancient World* (Eds D.M. Martill, G. Bechly and R.F. Loveridge), pp. 79–96. Cambridge University Press, Cambridge.

Meyer, H.W. and **Smith, D.M.** (Eds) (2008). *Paleontology of the Upper Eocene Florissant Formation, Colorado, GSA Special Paper*, Vol. 435, 177 pp.

Moshier, S.O. (1989) Microporosity in micritic limestones: a review. *Sed. Geol.*, **63,** 191–213.

Neumann, V.H., Borrego, A.G., Cabrera, L. and **Dino, R.** (2003) Organic matter composition and distribution through the Aptian-Albian lacustrine sequences of the Araripe Basin, northeastern Brazil. *Int. J. Coal Geol.*, **54,** 21–40.

Paz, J.D.S. and **Rossetti, D.F.** (2006) Paleohydrology of an Upper Aptian lacustrine system from northeastern Brazil: integration of facies and isotopic geochemistry. *Palaeogeogr. Palaeoclimatol. Palaeoecol.*, **241,** 247–266.

Ponte, F.C. and **Appi, C.J.** (1990). Proposta de revisão do coluna litoestratigrafica da bacia do Araripe. In: *36e Congresso Brasileiro de Geologica*. pp. 211–226, Natal.

Ponte, F. and **Ponte Filho, F.** (1996). Evoluçao tectonica e classificação da Bacia do Araripe. In: *Boletim do 4°* Simpósio sobre o Cretáceo do Brasil UNESP, pp. 123–133. Campus de Rio Claro, São Paulo.

Ricketts, R.D. and **Johnson, T.C.** (1996) Early Holocene changes in lake level and productivity in Lake Malawi as interpreted from oxygen and carbon isotopic measurements from authigenic carbonates. In: *The Limnology, Climatology and Palaeoclimatology of the East Africa lakes* (Eds T.C. Johnson and E.O. Odada). pp. 475–493. Gordon and Breach, Amsterdam.

Schaller, T., Moor, H.C. and **Wehrli, B.** (1997) Sedimentary profiles of Fe, Mn, V, Cr, As and Mo as indicators of benthic redox conditions in Baldeggersee. *Aquat. Sci.*, **59,** 345–361.

Stabel, H.-H. (1986) Calcite precipitation in Lake Constance: chemical equilibrium, sedimentation, and nucleation by algae. *Limnol. Oceanogr.*, **31,** 1081–1093.

Staplin, F.L. (1982). Determination of thermal alteration index from color of exinite (pollen, spores). In: *How to Assess Maturation and Palaeotemperatures* (Ed. F.L. Staplin), *SEPM Short Course*, Vol. 7, pp. 7–11. Soc. Econ. Paleo. and Miner. Tulsa.

Stephenson, M.H., Leng, M.J., Michie, U. and **Vane, C.H.** (2006) Palaeolimnology of palaeozoic lakes, focussing on a single lake cycle in the Middle Devonian of the Orcadian Basin, Scotland. *Earth Sci. Rev.*, **75,** 177–197.

Szulc, J. and **Cwizewicz, M.** (1989) The Lower Permian fresh-water carbonates of the Slawkow Graben, southern Poland - Sedimentary facies context and stable isotope study. *Palaeogeogr. Palaeoclimatol. Palaeoecol.*, **70,** 107–120.

Talbot, M.R. (1990) A review of the paleohydrological interpretation of carbon and oxygen isotopic ratios in primary lacustrine carbonates. *Chem. Geol.*, **80,** 261–279.

Teranes, J.L., McKenzie, J.A., Bernasconi, S.M., Lotter, A.F. and **Sturm, M.** (1999) A study of oxygen isotopic fractionation during bio-induced calcite precipitation in eutrophic Baldeggersee, Switzerland. *Geochim. Cosmochim. Acta*, **63,** 1981–1989.

Thompson, J.B., Schultze-Lam, S., Berveridge, T.J. and **Des Marais, D.J.** (1997) Whiting events: biogenic origin due to the photosynthetic activity of cyanobacterial picoplankton. *Limnol. Oceanogr.*, **42,** 133–141.

Tribovillard, N.P. (1998) Cyanobacterially generated peloids in laminated, organic-matter rich, limestones: an unobtrusive presence. *Terra Nova*, **10,** 126–130.

Tucker, M.E. and **Wright, V.P.** (1990). *Carbonate Sedimentology*. Blackwell Scientific Publications, Oxford/London, 482 pp.

Wright, V.P., Alonso Zarza, A.M., Sanz, M.E. and **Calvo, J.P.** (1997) Diagenesis of Late Miocene micritic lacustrine carbonates, Madrid Basin, Spain. *Sed. Geol.*, **114,** 81–95.

Zhou, Z., Barrett, P.M. and **Hilton, J.** (2003) An exceptionally preserved Lower Cretaceous ecosystem. *Nature*, **421,** 807–814.

Ziegler, A.M., Eshel, G., McAllister Rees, P., Rothfus, T.A., Rowley, D.B. and **Sunderlin, D.** (2003) Tracing the tropics across land and sea: permian to present. *Lethaia*, **36,** 227–254.

Manuscript received 11 December 2008; revision accepted 14 September 2009